

Thermodynamical Properties of a Spin- $\frac{1}{2}$ Heisenberg Chain Coupled to Phonons

Rainer W. Kühne

Fachbereich Physik, Universität Wuppertal, 42097 Wuppertal, Germany

Ute Löw

Institut für Theoretische Physik, Universität Dortmund, 44221 Dortmund, Germany

We performed a finite-temperature quantum Monte Carlo simulation of the one-dimensional spin- $\frac{1}{2}$ Heisenberg model with nearest-neighbor interaction coupled to Einstein phonons. Our method allows to treat easily up to 100 phonons per site and the results presented are practically free from truncation errors. We studied in detail the magnetic susceptibility, the specific heat, the phonon occupation, the dimerization, and the spin-correlation function for various spin-phonon couplings and phonon frequencies. In particular we give evidence for the transition from a gapless to a massive phase by studying the finite-size behavior of the susceptibility. We also show that the dimerization is proportional to g^2/Ω for $T < 2J$.

PACS numbers: 75.10.Jm, 75.40.Mg, 75.50.Ee

I. INTRODUCTION

In this paper we study the finite-temperature properties ($T/J \geq 0.1$) of the spin- $\frac{1}{2}$ Heisenberg model coupled to (dispersionless) Einstein phonons,

$$\mathcal{H} = \frac{J}{2} \sum_{l=1}^N (\vec{\sigma}_l \vec{\sigma}_{l+1} - 1) (1 + g(b_l^\dagger + b_l)) + \Omega \sum_{l=1}^N b_l^\dagger b_l, \quad (1)$$

in the parameter range of the spin-phonon couplings $0 \leq g \leq 1.5$ and phonon frequencies $0.2 \leq \Omega/J \leq 20$.

The phenomenological interest in this model dates back to the fundamental work of Pytte¹ who showed that a spin- $\frac{1}{2}$ Heisenberg chain coupled to three-dimensional phonons undergoes a dimerization transition, generally referred to as “spin-Peierls” transition. Motivated by the discovery² of a transition of this type in the inorganic substance CuGeO₃, the model proposed by Pytte and its modifications have been widely studied in recent time. (Thus following a period when CuGeO₃ was mostly discussed in the framework of a frustrated and dimerized spin-Hamiltonian with a temperature-dependent dimerization as a relict of the spin-phonon coupling.) In particular the low-temperature properties of the model Eq. (1)

were evaluated recently by Lanczos and DMRG techniques in Refs. 3–7 and by a continuous time world-line Monte Carlo algorithm in Ref. 8. At $T \neq 0$ a stochastic series expansion Monte Carlo was performed in Ref. 9.

In this paper we are mostly concerned with the finite-temperature properties of the model. We thus partly reproduce results of Ref. 9 where the model Eq. (1) was studied at finite T for $g = 1/(4\sqrt{2})$ and $\Omega = 0.2J$. In contrast to Ref. 9 we analyze in this work both the adiabatic limit of the model and also its gapless region where the thermodynamic observables are only slightly effected by the coupling to the phonons. We also calculate the specific heat, the spin-spin correlations and take advantage of the pronounced periodic patterns in the local phonon displacement to determine the parameter range where the model is dimerized. Our choice of parameters is motivated by Ref. 10 where the dominating phonon modes for CuGeO₃ are found to be $\Omega_1/J = 2$, $\Omega_2/J = 4$, $g_1 = -1/8$, and $g_2 = 1/2$.

The outline of the paper is as follows. In Sec. II we briefly describe the Monte Carlo loop algorithm we employed. In Sec. III we present the thermodynamic properties, in particular we demonstrate the presence of a phase transition from a gapless to a gapped phase by studying the finite-size behavior of the magnetic susceptibility. We also show the effect of the spin-phonon coupling on the specific heat and discuss results for the phonon occupation number. In Sec. IV we consider the local phonon displacement operator and determine the approximate boundary of the dimerized phase of the model. We study the dependence of the effective coupling J_{eff} on Ω and g and finally find an interesting crossover in the spin-spin correlations between the high and low-temperature phase. Conclusions are given in Sec. V.

II. QUANTUM MONTE CARLO METHOD

For this work we developed an extension of the quantum Monte Carlo loop algorithm^{11,12}. Like for the world-line method the key idea of the loop algorithm is a mapping of the partition function of a n -dimensional quantum spin system onto a $(n+1)$ -dimensional classical system. However, its substantial advantage is that compared to the world-line method it allows global spin updates, thus substantially reducing the autocorrelation times. Also the variation of both winding number and magnetization are automatically included.

For our simulation we used two Trotter layers for the spin-spin and the spin-phonon part of H and introduced a third layer for the free phonon part. We then combined global loop updates for the spin-phonon and spin-spin coupling with local heat bath updates modifying the phonon occupation number. It is obvious that detailed balance is satisfied for the two steps and thus also for the whole procedure. The decomposition of the partition function which forms the basis of our calculation is given in the appendix.

We studied chains with 16 up to 128 sites using typically $10^5 \dots 10^6$ spin updates for each temperature. Even though the importance sampling technique was employed for the phonon update, its acceptance rate is still smaller than that of the spin update. Best results were obtained by making ≈ 20 phonon updates per spin update and using only the last of the phonon updates for the evaluation of the expectation values. Also for each temperature the first 10% of all the sweeps were used for thermalization. We find that the measured quantities depend linearly on the inverse Trotter number squared. This can be seen in Fig. 1, where we show the susceptibility for a $N = 16$ system and Trotter number $M = 10, \dots, 80$ as function of $1/M^2$. In the present work we either extrapolated our results in the Trotter number, according to the above law, or when we found the fluctuations to be larger than the effect of the finite Trotter number, we gave the explicit value of the Trotter number in the figures.

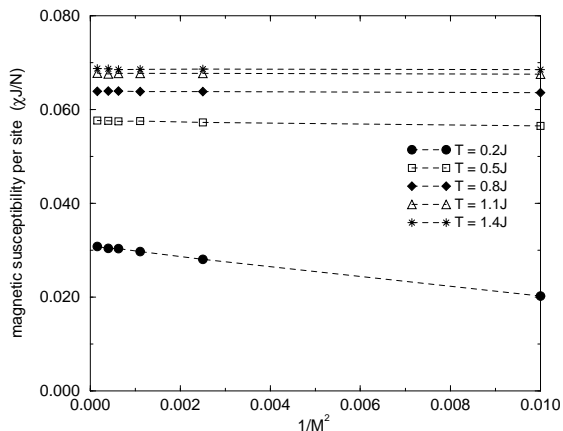


FIG. 1. Magnetic susceptibility for temperatures $T/J = 0.2, 0.5, 0.8, 1.1, 1.4$ as a function $1/(\text{Trotter number})^2$ for $N = 16$ spins, phonon frequency $\Omega = J$, and spin-phonon coupling constant $g = 0.2$.

III. THERMODYNAMIC PROPERTIES

A. Magnetic Susceptibility

It is known that the magnetic susceptibility of CuGeO_3 in the temperature range above the spin-Peierls tran-

sition can be well fitted by a frustrated Heisenberg model^{13–15}. It is often objected, however, that the excellent agreement of theory and experiment is accidental, since it does not take into account interchain interactions and spin-phonon couplings. Motivated by this controversy we pursue the question to what extent the spin-phonon coupling influences the susceptibility.

We summarize our observations on the high-temperature properties of the susceptibility in the following three points.

(i) For fixed phonon frequency, the overall height of the susceptibility is lowered with an increasing spin-phonon coupling (Fig. 2).

(ii) For fixed g , the susceptibility is growing and its maximum is shifted to lower temperatures with increasing frequency Ω (Fig. 3).

(iii) As the spin-phonon coupling is increased the maxima of the susceptibility curves are shifted to higher temperatures.

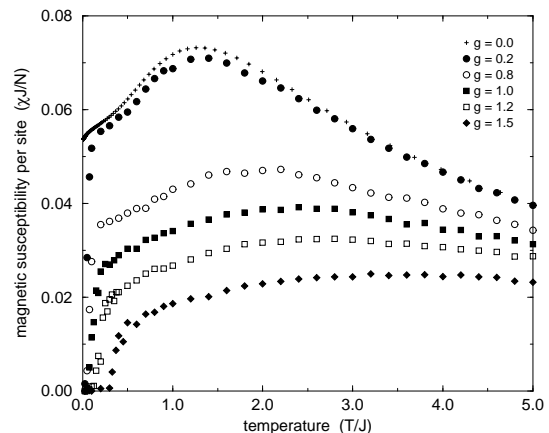


FIG. 2. Magnetic susceptibility versus temperature for $\Omega = 2J$ and spin-phonon coupling g between 0.2 and 1.5. The number of sites is $N = 64$ for low temperatures, $T \leq J$, and $N = 16$ for high temperatures. For comparison we show the exact results for the Heisenberg model calculated by A. Klümper¹⁶ via the quantum transfer matrix approach.

Point (i) is not surprising, since an increase of the spin-phonon coupling is expected to decrease the magnetic order. Point (ii) can be explained by the fact that for $\Omega \gg gJ$ the magnetic and phononic degrees of freedom decouple. So for $\Omega \rightarrow \infty$ (and gJ fixed) the magnetic properties are again dominated by the antiferromagnetic Heisenberg model. Point (iii) is of some phenomenological consequence because it means that for a substance where the spin-phonon coupling cannot be neglected, the value of the spin-spin coupling is overestimated, if determined by comparing the experimental data with the susceptibility calculated in a pure spin model. (We assumed that J is determined by matching temperatures where the experimental and theoretical susceptibility curves

have their maxima, which is a standard procedure, see for example Ref. 15.)

Also it should be noted that for frustrated models T_{max}/J is shifted to lower temperatures with increasing frustration parameter, i. e. the effect of the spin-phonon coupling is opposite to that of frustration. Together with the argument given in Section IV B it is obvious that the susceptibility of CuGeO_3 cannot be fitted with a model of the type Eq. (1).

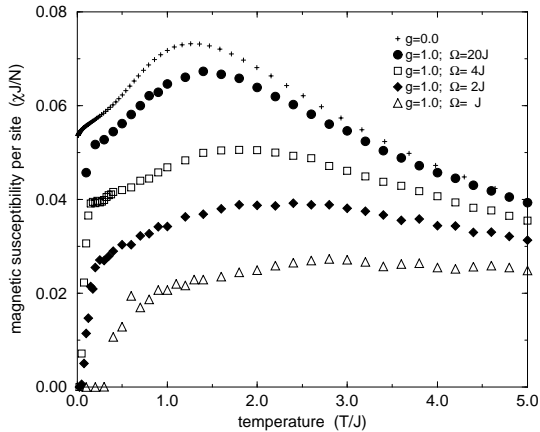


FIG. 3. Magnetic susceptibility versus temperature for $g = 1.0$ and phonon frequency between $\Omega = J$ and $\Omega = 20J$. The number of sites is $N = 64$ for low temperatures, $T \leq J$ ($T \leq 1.5J$ for the $\Omega = J$ chain), and $N = 16$ for high temperatures. For $g = 0$ we show the exact result from Ref. 16.

To draw definite conclusions from the susceptibilities at low T , finite-size effects have to be studied carefully.

In Fig. 4a we show results for $\Omega = 2J$ and $g = 0.5$ and chain lengths $N = 16, 32, 64, 128$. The tendency of the susceptibility curves is to approach a finite value at $T \rightarrow 0$. Thus the sharp decrease in the curves for $N = 16, 32, 64$ is a finite-size effect, i.e. the energy gap causing the drop is due to the discreteness of the spectrum of the finite system, it is not an intrinsic property of the spin chain (Fig. 4a).

The situation is drastically changed if we consider $g = 1.5$ and $\Omega = J$ (lower curve in Fig. 4b). Here the drop is unchanged when going to larger systems. This means that the gap in the spectrum is larger than the gap generated by the finite size of the chain. The upper curve in Fig. 4b shows results for $g = 0.8$ and $\Omega = J$, which exhibit clear finite-size effects but where the nature of the gap cannot be determined from systems of size $N \leq 128$. Since for $g = 0$ the model is gapless and in the adiabatic limit the model is known to be massive, the finite-size behavior shown in Fig. 4b gives clear evidence that the transition between the two phases occurs at finite g . This transition to a gapped phase is a signature of the lattice distortion. Indeed we will show in section IV A, that in the gapped phase we find well developed

dimerization patterns at low T .

The existence of this phase transition has been previously reported at $T = 0$ in Ref. 8 where by means of a continuous time world-line algorithm it is shown that a critical coupling between gapless and spin-fluid phase exists for a fixed Ω . Also for a model with a slightly different spin-phonon coupling the phase diagram was determined in Ref. 17 by means of DMRG technique and for a model including a frustrating spin-spin coupling evidence for the transition can be found in Ref. 5.

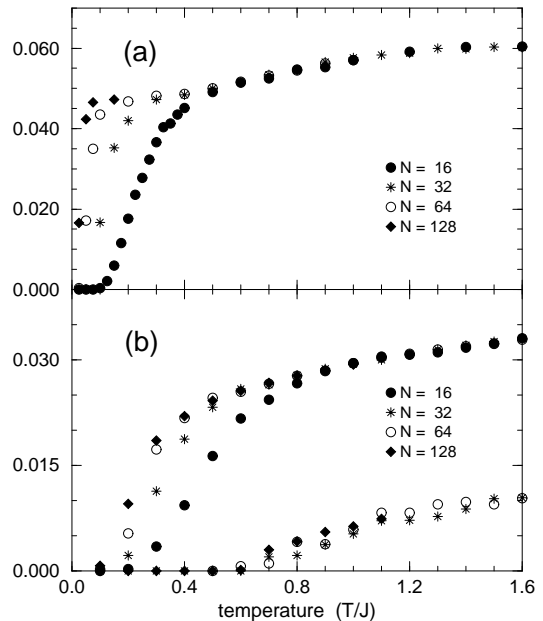


FIG. 4. Finite-size behavior of the magnetic susceptibility. The upper figure shows a chain with phonon frequency $\Omega = 2J$ and spin-phonon coupling constant $g = 0.5$, the lower figure shows chains with $\Omega = J$ and $g = 0.8$ (upper curve) and $g = 1.5$ (lower curve).

B. Specific Heat, Phonon Occupation Number

The idea to get further information about magnetic properties by considering besides the susceptibility also the specific heat suggests itself since the specific heat is an observable, that can be as easily measured and calculated as the susceptibility. However, in practice only for substances with very small J (Cu(L-alanine)_2 with a $J = 0.55\text{K}$ for example¹⁸) the specific heat can be directly

compared with experiment. For most of the inorganic substances (in particular for CuGeO_3) which have spin-spin couplings of the order of 100K, lattice vibrations dominate the specific heat and it is an unsolved problem to extract its magnetic part. As a first approximation¹⁹ it was assumed for CuGeO_3 that it is sufficient to subtract the contribution of the phonons and consider the rest as the contribution of the spins. We show that such an approximation is not justified even in the simple case of dispersionless phonons.

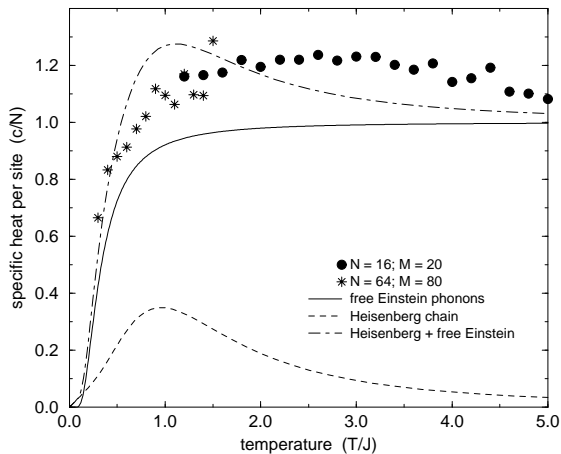


FIG. 5. Temperature-dependence of the specific heat for a chain with phonon frequency $\Omega = J$ and spin-phonon coupling constant $g = 1.0$. The number of sites is 16 and 64, respectively.

To demonstrate this we plot in Fig. 5 the specific heat c for a chain with $\Omega = J$ and $g = 1.0$ together with the specific heat c_f of the free Einstein phonons

$$c_f = \left(\frac{\Omega}{T}\right)^2 \frac{e^{\Omega/T}}{(e^{\Omega/T} - 1)^2}, \quad (2)$$

with $\Omega = J$ and the contribution c_H of the isotropic Heisenberg model¹⁶. As can be clearly seen the Einstein phonons are dominant at high temperatures, in particular the constancy of the specific heat, as expected according to the Dulong-Petit rule, is visible. However, also the effect of the spin-phonon coupling can be perceived, since we find that the maximum at $T \approx J$ of the $c_f(T) + c_H(T)$ (dot-dashed line) becomes less pronounced and is shifted toward higher temperatures by the presence of the spin-phonon coupling. When going to larger frequencies (and g fixed), the contribution of the spin-phonon coupling decreases, but only for $\Omega \geq 4J$ and $g = 1.0$ we find that $c(T)$ can be approximated by $c_f(T) + c_H(T)$. Of course when considering the specific heat the phonon dispersion, which is not taken into account, is most important and more work on realistic models is needed to compare the-

oretical results in a quantitative way with experimental data.

Further insight in the model can be gained, by studying to what extent the phonon-occupation number is influenced by the spin-phonon coupling.

$$n(T) = \frac{1}{N} \sum_{l=1}^N \langle b_l^\dagger b_l \rangle. \quad (3)$$

We first consider $\Omega = 4J$ and $g = 1$, parameters for which we found above that the specific heat can be approximated without the spin-phonon coupling. For $n(T)$ we find in this case that the effect of the spin-phonon coupling is solely to shift the contribution

$$n_f(T) = \frac{1}{e^{\Omega/T} - 1} \quad (4)$$

of the free phonons by a constant value n_0 (see Fig. 6). We determined from the low temperature data that $n_0 = 2(gJ/\Omega)^2$, which in agreement with Ref. 7 where this relation was found for a chain with a single $k = \pi$ phonon mode. However, for $g = 1$ and $\Omega/J = 1, 2$ deviations from the free phonon case become visible. In particular the slope of $n(T)$ at high T is substantially smaller than $1/\Omega$. Also the constant shift deviates from $2(gJ/\Omega)^2$. Note that the drop of $n(T)$ at low T is an effect of both finite Trotter number and the finite size of the system.

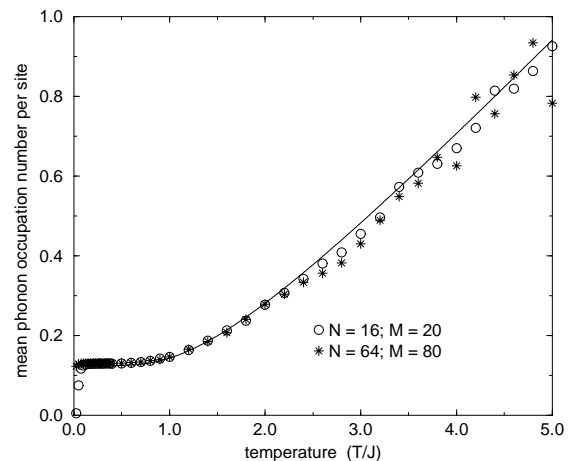


FIG. 6. Mean phonon occupation number as a function of temperature for phonon frequency $\Omega = 4J$ and spin-phonon coupling constant $g = 1.0$. The number of sites is 16 and 64, respectively. The solid line shows $n_f(T) + n_0(T)$, where $n_0(T) \equiv n(T) - n_f(T)$ was approximated by the temperature-independent value $n_0(0) = 2(gJ/\Omega)^2$.

We conclude this section with a more technical remark concerning truncation errors. As the dimension of the subspaces is quickly growing with the number of phonons the limits of a method requiring truncation is

soon reached, this is relevant when using exact diagonalization which allows to treat only ≈ 16 spins and a few phonons per site. At zero temperature the truncation problem can be partly overcome by using coherent phonon states^{4,20} or employing the DMRG technique, which allows to treat system sizes of up to 256 spins¹⁷. At finite temperatures, however, the truncation problem is even more important. With the probability distribution of the phonon occupation number shown in Fig. 7 we dramatically demonstrate that high cutoffs are essential when studying finite temperature properties. For the correct treatment of a chain with $\Omega \geq J$ and $g = 1.0$ at $T = J$ a truncation at ≈ 30 spins is needed (as can be seen from the figure the probability for more than 28 phonons per site is less than 10^{-7}). For $\Omega/J = 0.5$ the truncation is ≤ 50 spins/site and only very high phonon frequencies as $\Omega/J = 20$ can be treated with 4 phonons per site.

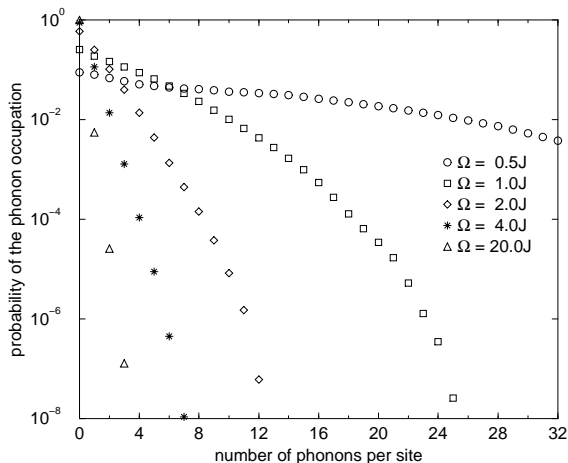


FIG. 7. Probability of the phonon occupation number for phonon frequencies between $\Omega/J = 0.5$ and 20 for a chain with $N = 64$ sites, Trotter number 80, spin-phonon coupling constant $g = 1.0$, and temperature $T = J$.

IV. DIMERIZATION AND SPIN-CORRELATIONS

Addressing now the question of the dimerization, we expect that the ground state of the model Eq. (1) in the massive phase shows short range correlations and strong signatures of dimerization. We extract the boundaries of the phase diagram in the g - Ω plane by studying the dimerization patterns at low temperatures and corroborate the results by considering the divergence of the structure factor at $q = \pi$. We also give account of the averaged phonon displacement often referred to as an “effective coupling”, which is nonzero for all $g \neq 0$ and $\Omega \neq 0$.

A. Dimerization

To begin, let us recall the definition of the local phonon displacement operator

$$\delta_l = g \langle b_l^\dagger + b_l \rangle \quad (5)$$

which corresponds in the adiabatic limit to the dimerization in a Heisenberg model with alternating couplings. Its average over all sites l ,

$$\delta = \frac{1}{N} \sum_{l=1}^N \delta_l, \quad (6)$$

represents the uniform phonon displacement and is closely related to the effective spin-spin coupling^{1,9}

$$J_{\text{eff}} = J(1 + \delta). \quad (7)$$

It is well-known that in spin-Peierls substances like CuGeO_3 the transition from the uniform to the dimerized phase occurs at finite temperatures, here however, we consider a strictly one-dimensional model with a dimerization transition at $T = 0$. So to encounter dimerization one needs to go to temperatures as low as possible.

By studying δ_l at low temperatures in the parameter range $0 \leq \Omega/J \leq 3$ and $0 \leq g \leq 2$ we can clearly distinguish two different phases of the model. We find either pronounced periodic patterns in δ_l (see Fig. 8) or random fluctuations with no perceivable periodicity down to temperature $T/J = 0.05$. We note that as T is risen to higher temperatures the periodic patterns weaken and at higher T domains of periodic fluctuation are perceivable, which reflect a “reminiscence” of the periodic fluctuations present at $T = 0$ (see second and third graph of Fig. 8).

It is of interest to see how the periodic patterns in the phonon displacement are connected with the formation of spin-dimers. So to complete the picture we calculated the local spin-spin correlations $\langle \vec{\sigma}_l \cdot \vec{\sigma}_{l+1} \rangle$. We find that the periodic patterns in the local displacement δ_l are well in phase with the formation of spin singlet states, which demonstrates the coupling of the phononic degrees of freedom and the spin degrees of freedom. This is also an *á posteriori* check of the consistency of our combined spin and phonon updates. (see the lowest three graphs of Fig. 8. As can be seen from the Fig. 8 the dimerization is not complete, since the correlation between the singlet states is not zero.)

Thus δ_l proves to be a valuable tool, which allows more easily than the susceptibility to decide, for fixed parameter values whether the model is in a dimerized state.

We use this property to determine the approximate phase boundaries in the $g - \Omega$ plain. To be concrete, we calculated δ_l for a 64 site system at temperatures $T/J = 0.4, \dots, 0.1$ and inferred from the periodic fluctuations the phase diagram shown in Fig. 9. Since for all

points δ_l either shows random patterns or the periodic fluctuations, we can unambiguously determine, whether the model at a certain point in parameter space is in a dimerized phase. We cannot however state definitely, that the model is gapless if we encounter no dimerization, because we are limited both in system size and temperature. So rigorously the separation line between the two phases in Fig. 9 gives the minimal extension of the dimerized phase, i.e. in the thermodynamic limit the dimerized phase will be larger and the separation line in Fig. 9 will be shifted to the left. Comparing with the results of Fig. 4 we find that the point $g = 1.5$ and $\Omega = J$ where from the susceptibility we found that the model must be in a massive phase shows clear patterns of dimerization, and the point $g = 0.8$ and $\Omega = J$, for which the finite size argument was not conclusive, turns out to be in the dimerized phase.

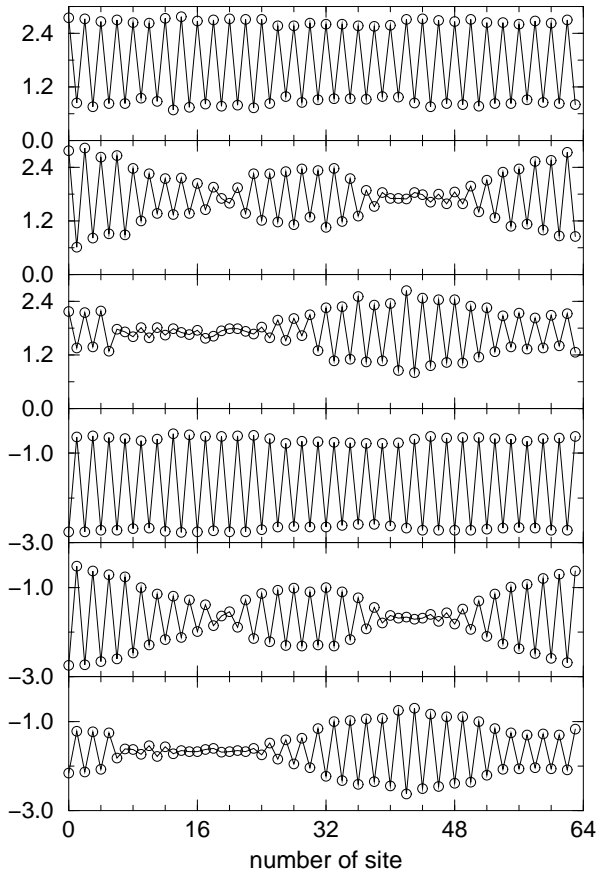


FIG. 8. Upper three graphs: local displacement $\langle b_l^\dagger + b_l \rangle$ for $T = 0.3J, 0.4J, 0.5J$. Lower three graphs: spin-spin-correlation $\langle \vec{\sigma}_l \cdot \vec{\sigma}_{l+1} \rangle$ for the same temperatures. All graphs are for $N = 64$, $M = 80$, $\Omega = 2J$, $g = 1.5$, and averaged over 10,000 spin updates.

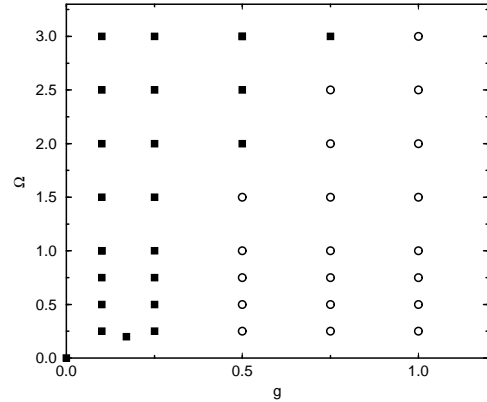


FIG. 9. Phase-diagram of the model in the g - Ω plain. Circles mark points with dimerization, squares points where no dimerization was found for $N = 64$ and $T \geq 0.1J$.

B. Effective coupling J_{eff}

We turn now to the averaged quantity δ and study the effective coupling J_{eff} as given by Eq. (7). It is worth noting that both in the dimerized and the undimerized phase δ is nonzero i.e. the spin-spin coupling is always shifted by the presence of the spin-phonon coupling. Our analysis shows that for all choices of parameters J_{eff} is a slowly decreasing function of temperature (Fig. 10), this behavior has been noted before for $g = 1/(4\sqrt{2})$ and $\Omega = 0.2J$ in Ref. 9.

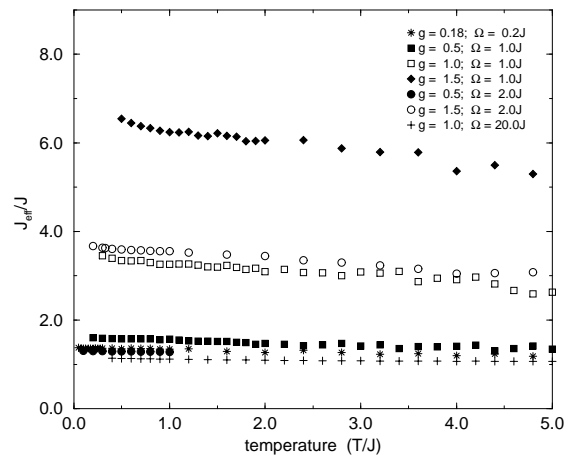


FIG. 10. Effective spin-coupling J_{eff}/J versus temperature.

From the phenomenological point it is interesting that a lowering of J with temperature is in agreement with Ref. 21 where a comparison of inelastic neutron scattering data on CuGeO_3 with calculated dynamic structure

factors $S(q, \Omega)$ gave evidence for a decrease of J with increasing temperature. A similar behavior of J has been reported in Ref. 22.

With our results for J_{eff} we are in the position, to study the question to what extent J_{eff} is an effective coupling in the proper sense, in other words, whether it can be used to rescale the thermodynamic quantities in such a way that the results for the Heisenberg model are regained. We find that the rescaled susceptibilities $\chi(T)J_{\text{eff}}(T)$ plotted versus temperature as shown in Fig. 11 do not fall together with the curves of the Heisenberg model. So one is forced to conclude that the effective coupling cannot be used to bring the curves with different parameter together. One cannot infer from this however, that essential new physics – maybe a sign of a frustration – is perceivable. The above result means only that J_{eff} is not the correct variable to rescale the thermodynamical observables.

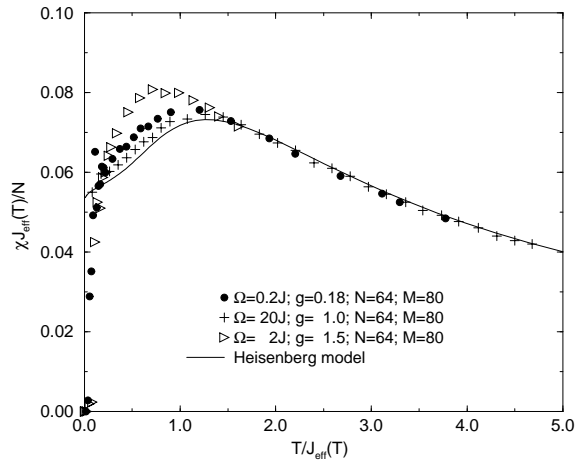


FIG. 11. Rescaled susceptibilities $\chi(J, g, T, \Omega) J_{\text{eff}}(T) / N$ versus $T / J_{\text{eff}}(T)$

On the other hand we find that to high precision the susceptibilities (for not too low T) can be rescaled by a global and temperature independent J_{eff}^g / J (Fig. 12). That is we find

$$\chi(J, g, T, \Omega) J_{\text{eff}}^g = J \chi^{\text{AFH}}(T / J_{\text{eff}}^g, J_{\text{eff}}^g) \quad (8)$$

where J_{eff}^g is a global effective coupling, which we determined by comparing the temperatures T_{max} where the susceptibilities of the Heisenberg model and the model Eq. (1) have their maxima

$$J_{\text{eff}}^g = J \frac{T_{\text{max}}(g, \Omega)}{T_{\text{max}}^{\text{AFH}}} \quad (9)$$

We note that there is a discrepancy to Ref. 9 where an overall g -Factor was required to obtain a similar scaling law.

This scaling of the susceptibilities is of phenomenological importance also for CuGeO_3 , since it is well known that the susceptibility of a frustrated model^{13,15} cannot be mapped by a rescaling of J onto that of the Heisenberg model. This lends further evidence to the argument given in Sec. III A that no agreement with the experimental susceptibility of CuGeO_3 can be achieved. By checking with data from the model with frustration we estimate that a frustration parameter of ≈ 0.12 might go undetected in our analysis, because the statistical fluctuations hide the small effect on χ for frustrations less than 0.12.

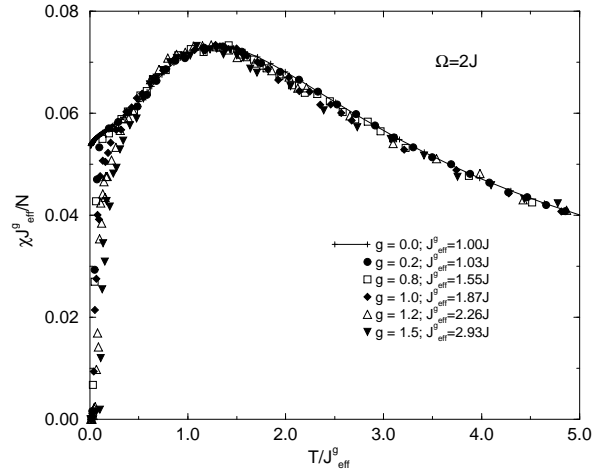


FIG. 12. Rescaled susceptibilities $\chi(J, g, T, \Omega) J_{\text{eff}}^g / N$ versus T / J_{eff}^g

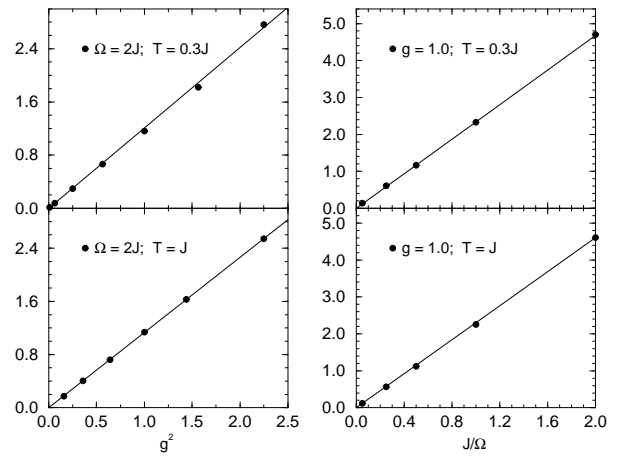


FIG. 13. Displacement $\delta = J_{\text{eff}} / J - 1$ versus g^2 (left side) and versus J / Ω (right side) for $N = 64$ and Trotter number $M = 80$.

As a last point we show that δ is proportional to g^2/Ω in the temperature range $T < 2.0J$, (see Fig. 13). The constants of proportionality for the data shown in Fig. 13 are $c(T = 0.3J) = (2.38 \pm 0.04)J$ and $c(T = J) = (2.28 \pm 0.02)J$.) At higher temperatures we found deviations from the simple law. This result is in qualitative agreement with observations by Wellein et al.⁵, who found a lowering of the dimerization with growing frequency at $T = 0$, it also confirms calculations of Pytte¹ and Uhrig²³, who found the spin-phonon Hamiltonian (for translationally invariant phonons) equivalent to an effective spin Hamiltonian with spin-spin coupling $\propto g^2/\Omega$.

C. Correlations

With our method it is straightforward to calculate spin-spin-correlation functions $\langle \vec{S}_i \cdot \vec{S}_j \rangle$ as a function of temperature. We postpone a fit of the correlation functions in the strongly dimerized phase and a detailed discussion of the critical exponents in the gapless phase to a later publication and highlight at the end of this work the most spectacular features of the correlation functions only.

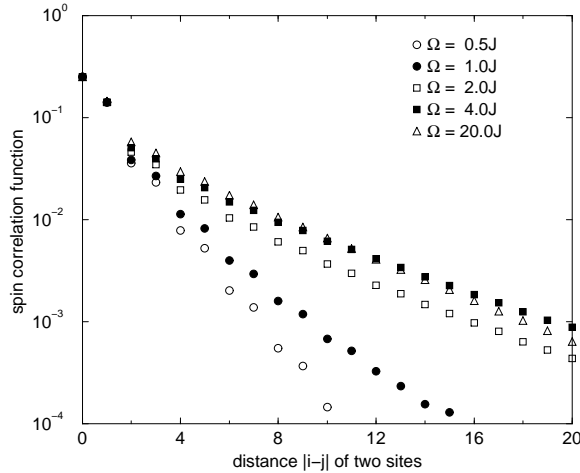


FIG. 14. $\langle \vec{S}_i \cdot \vec{S}_j \rangle (-1)^{i-j}$, as a function of distance for $g = 1.0$ for a 64 site chain, $M=80$, phonon frequency $\Omega = 0.5J, \dots, 20J$ at $T = 0.3J$.

(i) We find that the spin-spin correlations as a function of distance show a pronounced steplike behavior (see Fig. 14) in the gapped phase. This is again a signature of the dimerization of the ground state. (Note that for a completely dimerized state we would have one step only, however, we find a finite correlation between the dimers.)

(ii) For increasing Ω at fixed g one finds the correlations more and more unaffected by the spin phonon coupling,

which is due to the decoupling of spins and phonons as we observed before when studying the susceptibility.

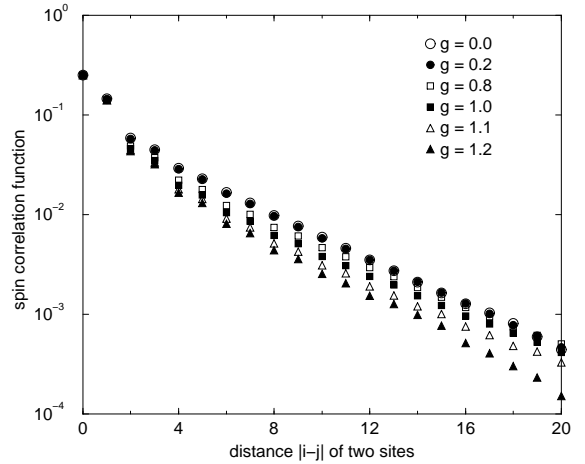


FIG. 15. Spin-spin correlation $\langle \vec{S}_i \cdot \vec{S}_j \rangle (-1)^{i-j}$, as a function of distance for $g = 0, \dots, 1.2$ for a 64 site chain, $M=80$, phonon frequency $\Omega = 2J$ at $T = 0.3J$.

(iii) As a function of g we observe a crossover between the high-temperature and the low-temperature range. At low temperatures the correlations decrease with growing spin-phonon coupling (Fig. 15). This is analogous to the dimerized model where one finds a lowering of the correlation with growing dimerization. For high temperatures, however, the inverse behavior occurs: the correlations for $g = 1.5$ are highest and for $g = 0.2$ are lowest. (For $\Omega = 2J$ the transition between low and high-temperature region occurs at $T = (0.55 \pm 0.05)J$.)

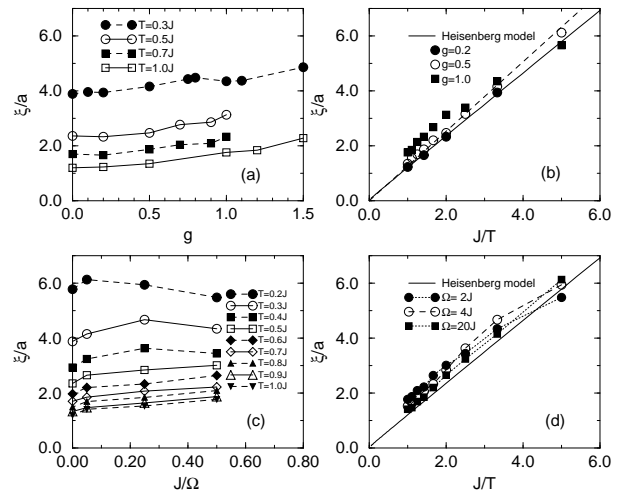


FIG. 16. Correlation length ξ in lattice units a for $\Omega = 2J$ (upper figures) and $g = 1.0$ (lower figures). The chain length is $N = 64$ and the Trotter number $M = 80$.

(iv) In the gapless region of the model the correlations decay exponentially with a correlation length that coincides for $g \leq 0.2$ with the known Heisenberg result

$$\xi(T) = cT^{-\nu} \quad \text{with } \nu = 1 \text{ for } N \rightarrow \infty \quad (10)$$

(see Fig. 16b). For larger g we encounter deviations from Eq. (10) which can best be fitted by allowing ν to differ from 1. (e. g. $\nu = 0.92$ for $g = 0.5$ and $\Omega = 2J$). In Fig. 16a,c we show ξ as a function of g and $\frac{1}{\Omega}$. We find that for temperatures $0.5 < T/J < 1$ the correlation length ξ decreases slightly with g and $\frac{1}{\Omega}$. However, a more careful investigation is needed to give conclusive evidence for the functional dependence of $\xi(g, \Omega, T) = c(g, \Omega)T^{-\nu(g, \Omega)}$.

(v) The pronounced maxima of the static structure factor $S(q, T)$ at $q = \pi$ for $g = 0$ as shown in Fig. 17 originate from the logarithmic divergence of $S(q, T = 0)$ of the isotropic Heisenberg model. (For a study as to what extent this divergence can be seen at finite T we refer to Ref. 24.) For the model Eq. (1) in the gapless phase the peak in $S(q)$ at $q = \pi$ is only slightly diminished as compared to the Heisenberg model, indicating that the models show a similar divergent behavior. On the contrary in the gapped phase the structure factor shows a broad maximum hinting toward a regular behavior of $S(q = \pi, T = 0)$.

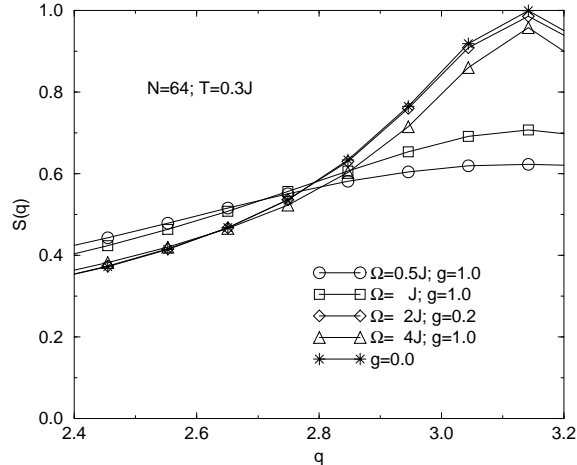


FIG. 17. Structure factor $S(q)$ versus momentum q .

V. CONCLUSIONS

We have developed a modified quantum Monte Carlo loop algorithm to study the finite-temperature properties of the one-dimensional isotropic antiferromagnetic Heisenberg model coupled to Einstein phonons. We have investigated in detail the magnetic susceptibility, specific

heat, phonon occupation number, dimerization, and spin-correlation for chains with 16 up to 128 sites down to temperatures $T = 0.05J$.

We found evidence for a phase transition from a gapless to a massive phase and used the periodic fluctuations in the local displacement to determine the approximative phase diagram of the model. Furthermore, the dimerization patterns we encountered were accompanied by the formation of spin singlet states.

The temperature-dependence of the effective spin-spin coupling J_{eff} was calculated and it was shown that $J_{\text{eff}}(T) = (1 + c(T)g^2/\Omega)J$, for $T/J \leq 2.0$.

At low temperatures the mean phonon occupation number was found to be proportional to the square of the spin-phonon coupling constant and inversely proportional to the square of the phonon frequency.

We demonstrated that the susceptibility of CuGeO_3 cannot be described by the model.

VI. ACKNOWLEDGEMENT

We thank K. Fabricius for his continuous and stimulating interest in our work. We are grateful to A. Fledderjohann, G. Uhrig, W. Weber, and R. Werner for valuable discussions. The support of the Deutsche Forschungsgemeinschaft and the Graduiertenkolleg Wuppertal is acknowledged.

VII. APPENDIX

The Trotter decomposition of the partition function Z we used as basis of our quantum Monte Carlo method reads:

$$Z = \lim_{M \rightarrow \infty} \sum_{k_0, \dots, k_{3M-1}} \prod_{j=0}^{M-1} \left(\prod_{l=0}^{N-1} \langle k_{3j,l} | e^{-\beta \Omega (b_l^\dagger b_l)/M} | k_{3j+1,l} \rangle \right) \left(\prod_{l=0}^{N/2-1} \langle k_{3j+1,2l} | e^{-\beta \mathcal{H}_{2l}/M} | k_{3j+2,2l} \rangle \right) \langle k_{3j+2,2l+1} | e^{-\beta \mathcal{H}_{2l+1}/M} | k_{3j+3,2l+1} \rangle. \quad (11)$$

k denotes the spin and phonon configurations of the lower and upper edge of the interacting plaquettes, the inverse temperature is β , the Trotter number M , and the Hamiltonian for the spin-spin and the spin-phonon interaction is

$$\mathcal{H}_l = \frac{J}{2} (\vec{\sigma}_l \vec{\sigma}_{l+1} - 1) (1 + g(b_l^\dagger + b_l)). \quad (12)$$

-
- ¹ E. Pytte, Phys. Rev. B **10**, 4637 (1974).
- ² M. Hase, I. Terasaki, and K. Uchinokura, Phys. Rev. Lett. **70**, 3651 (1993).
- ³ D. Augier, D. Poilblanc, E. Sorensen, and I. Affleck, Phys. Rev. B **58**, 9110 (1998).
- ⁴ D. Augier, P. Hansen, D. Poilblanc, J. Riera, and E. Sorensen, cond-mat/9807265.
- ⁵ G. Wellein, H. Fehske, and A. P. Kampf, Phys. Rev. Lett. **81**, 3956 (1998).
- ⁶ A. Weiße, G. Wellein, and H. Fehske, cond-mat/9901262.
- ⁷ D. Augier and D. Poilblanc, Eur. Phys. J. B **1**, 19 (1998).
- ⁸ A. W. Sandvik and D. K. Campbell, cond-mat/9902230.
- ⁹ A. W. Sandvik, R. R. P. Singh, and D. K. Campbell, Phys. Rev. B **56**, 14510 (1997).
- ¹⁰ R. Werner, C. Gros, and M. Braden, cond-mat/9810038.
- ¹¹ H. G. Evertz, G. Lana, and M. Marcu, Phys. Rev. Lett. **70**, 875 (1993).
- ¹² H. G. Evertz, in *Numerical Methods for Lattice Quantum Many-Body Problems*, edited by D. J. Scalapino (Addison Wesley, Reading), to be published (= cond-mat/9707221).
- ¹³ G. Castilla, S. Chakravarty, and V. J. Emery, Phys. Rev. Lett. **75**, 1823 (1995).
- ¹⁴ J. Riera and A. Dobry, Phys. Rev. B **51**, 16098 (1995).
- ¹⁵ K. Fabricius, A. Klümper, U. Löw, B. Büchner, G. Dhalenne, T. Lorenz, G. Dhalenne, and A. Revcolevschi, Phys. Rev. B **57**, 1102 (1998).
- ¹⁶ A. Klümper, Z. Phys. B **91**, 507 (1993).
- ¹⁷ R. J. Bursill, R. H. McKenzie, and C. J. Hamer, cond-mat/9812409.
- ¹⁸ R. E. Rapp, E. P. de Souza, H. Godfrin, and R. Calvo, J. Phys.: Condens. Matter **7**, 9595 (1995).
- ¹⁹ M. Weiden, J. Köhler, G. Sparn, M. Köppen, M. Lang, C. Geibel, and F. Steglich, Z. Phys. B **98**, 167 (1995).
- ²⁰ R. Fehrenbacher, Phys. Rev. B **49**, 12230 (1994).
- ²¹ K. Fabricius and U. Löw, Phys. Rev. B **57**, 13371 (1998).
- ²² G. S. Uhrig, Phys. Rev. Lett. **79**, 163 (1997).
- ²³ G. S. Uhrig, Phys. Rev. B. **57**, R14004 (1998).
- ²⁴ K. Fabricius, U. Löw, and K.-H. Mütter, Phys. Rev. B. **51**, 8270 (1995).